ACS APPLIED MATERIALS & INTERFACES

Research Article

www.acsami.org

Boosting the Photocurrent Density of p-Type Solar Cells Based on Organometal Halide Perovskite-Sensitized Mesoporous NiO Photocathodes

Huan Wang,[†,⊥] Xianwei Zeng,[†,⊥] Zhanfeng Huang,[†] Wenjun Zhang,[†] Xianfeng Qiao,[†] Bin Hu,[†,‡] Xiaoping Zou,[§] Mingkui Wang,[†] Yi-Bing Cheng,[†,∥] and Wei Chen*[,†]

[†]Michael Grätzel Centre for Mesoscopic Solar Cells, Wuhan National Laboratory for Optoelectronics, Huazhong University of Science and Technology, Wuhan 430074, China

[‡]Department of Materials Science and Engineering, University of Tennessee, Knoxville, Tennessee 37996, United States

[§]Research Center for Sensor Technology, Beijing Key Laboratory for Sensors, School of Applied Sciences, Beijing Information Science and Technology University, Beijing 100192, China

[∥]Department of Materials Engineering, Monash University, Melbourne, Victoria 3800, Australia

Supporting Information

ABSTRACT: The p−n tandem design of a sensitized solar cell is a novel concept holding the potential to overcome the efficiency limitation of conventional single-junction sensitized solar cells. Significant improvement of the photocurrent density (J_{sc}) of the p-type half-cell is a prerequisite for the realization of a highly efficient p−n tandem cell in the future. This study has demonstrated effective photocathodes based on novel organometal halide perovskite-sensitized mesoporous NiO in liquid-electrolyte-based p-type solar cells. An acceptably high J_{sc} up to 9.47 mA cm^{-2} and efficiency up to 0.71% have been achieved on the basis of the $CH_3NH_3PbI_3$/NiO solar cell at 100 mW cm^{-2} light intensity, which are significantly higher than those of any previously reported liquid-electrolyte-based p-type solar cells based on sensitizers of organic dyes or inorganic quantum dots. The dense blocking layer made by spray pyrolysis of nickel acetylacetonate holds the key to determining the current flow direction of the solar cells. High hole injection efficiency at the perovskite/NiO interface and high hole collection efficiency through the mesoporous NiO network have been proved by time-resolved photoluminescence and transient photocurrent/photovoltage decay measurements. The limitation of these p-type solar cells primarily rests with the adverse light absorption by the NiO mesoporous film; the secondary limitation arises from the highly viscous ethyl acetate-based electrolyte, which is helpful for the solar cell stability but hinders fluent diffusion into the pore channels, giving rise to a nonlinear dependence of J_{sc} on the light intensity.

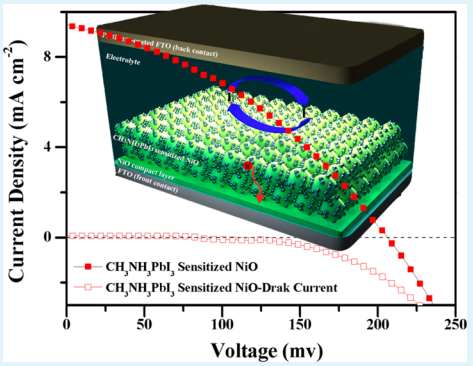

KEYWORDS: *sensitized solar cell, mesoporous NiO, perovskite, NiO blocking layer, p-type photocathode*

INTRODUCTION

The conventional dye-sensitized solar cells are based on n-type nanocrystalline TiO_2 photoanodes (n-DSCs), which have been intensively studied during the past 10−20 years.[1,2] The key components and photoconversion mechanism in such a solar cell system have attained a relatively mature stage.[3] Recently, novel p-type solar cells based on dye sensitization of p-type semiconductors (p-DSCs) have also attracted growing interest because they offer a new approach to converting solar energy into electricity[4−13] or chemical energy.[14,15] The cathodic photocurrent runs in the opposite direction compared to that of the conventional n-DSCs. What is more important, combining an efficient n-DSC and p-DSC can construct a p−n tandem DSC, which in principle has a theoretical efficiency upper limit of 43%,[4−6] certainly higher than that of single-junction solar cells and above the current efficiency record of an n-DSC (∼12%).[2] However, as a younger research field, sensitization of p-type semiconductors to date has not achieved satisfactory performance. The best p-DSC had only ∼0.5% efficiency.[11−13] As a consequence, the performance of p−n tandem DSCs was restricted at a low level.

Significant improvement of the photocurrent density (J_{sc}) of a p-DSC is a prerequisite for the realization of a highly efficient p−n tandem DSC in the future. Long after the concept of a p−n tandem DSC was first proposed by Lindquist et al. in 2000,[16] there is no significant progress in J_{sc} improvement of p-DSCs. More serious is that the principle of how to design the molecular structure of efficient dyes for a p-type semiconductor

Received: April 29, 2014
Accepted: June 27, 2014
Published: June 27, 2014

 © 2014 American Chemical Society dx.doi.org/10.1021/am5025963 | ACS Appl. Mater. Interfaces 2014, 6, 12609−12617

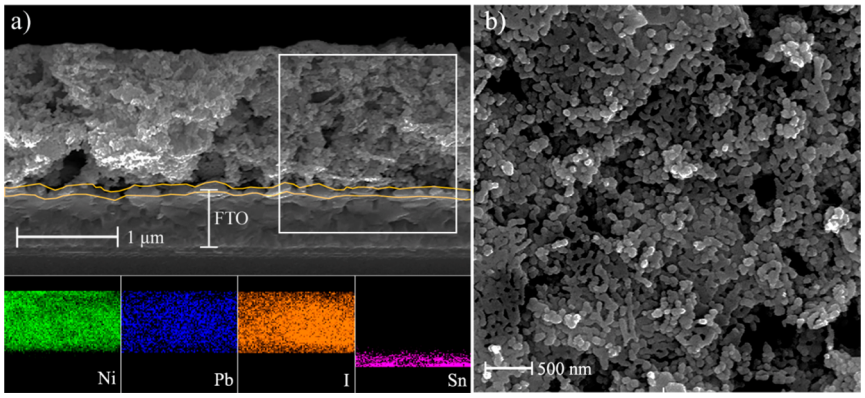

Figure 1. SEM images of a $CH_3NH_3PbI_3$-sensitized NiO film: (a) cross-section view and (b) top view. The insets at the bottom of (a) are EDX mapping results of the white square region. The yellow line highlights the compact NiO blocking layer.

remains unclear. This circumstance did not change until Hagfeldt and Sun et al. reported their first "donor−acceptor"-type dye (P1 dye) in 2008 to successfully sensitize nanocrystalline NiO.[8,9] In the P1 dye, the carboxylic acid anchoring group is smartly positioned on the electron donor part (triphenylamine), which benefits long-range separation of photogenerated charges and results in high incident photon-to-current efficiency (IPCE = 64%). The J_{sc} was then dramatically improved to 5.48 mA cm^{-2} after optimization of the mesoporous NiO film's morphology in 2010.[10] Besides these pioneering works, another work accomplished by Bauerle and Bach et al. in 2010 could be regarded as another big step for p-type dye development.[11] By tuning the length of the donor units (oligothiophene), the fast charge recombination between the photoinjected holes in NiO and electrons at the acceptor part of the p-type dye (PMI-6T-TPA dye) could be largely suppressed. A close to unit internal quantum efficiency or absorbed photon-to-current conversion efficiency (APCE = 96%) has been demonstrated by ignoring about 30−40% intrinsic light absorption of NiO. Their first reported J_{sc} was 5.35 mA cm^{-2}, which was subsequently improved to 7.0 mA cm^{-2} with a better NiO photocathode.[13] To the best of our knowledge, 7.0 mA cm^{-2} is the J_{sc} record of previously reported liquid-electrolyte-based p-DSCs.

More recently, several attempts have been made to substitute organic dyes with alternative inorganic sensitizers in p-type mesoscopic solar cells, such as metal chalcogenide quantum dots (QDs), to construct p-type QD-sensitized solar cells (p-QDSCs),[17−22] but the progress in this direction is even less. To the best of our knowledge, the best performance of liquid-electrolyte-based p-QDSCs was achieved on the basis of Se QD sensitization on a nanocrystalline TiO_2 film (might be a scaffold), with a J_{sc} of only 3.73 mA cm^{-2}.[17] Strong interfacial recombinations during charge carrier generation and collection processes should be responsible for the low J_{sc} of p-QDSCs.

In this study, we employed the newly emergent organometal halide perovskites $CH_3NH_3PbBr_3$ and $CH_3NH_3PbI_3$ to sensitize the mesoporous NiO photocathodes. By using the iodine-based liquid electrolyte, the $CH_3NH_3PbI_3$/NiO photocathode has achieved J_{sc} up to 9.47 mA cm^{-2}, which is dramatically improved compared to that of any previously reported liquid-electrolyte-based p-DSCs and p-QDSCs. Organometal halide perovskites as light absorbers have recently achieved great success in solid-state hybrid solar cells owning to their excellent properties, including low-temperature solution processability, suitable and direct band gaps, high absorption coefficient, etc.[23−31] The most unique feature should rest with the specific bipolar charge transport property; namely, both the photogenerated electrons and holes in the perovskites have high mobilities and lifetimes.[27,28] All of these results strongly encourage us to study the interesting p-type solar cells based on perovskite sensitizers. The perovskite-sensitized mesoporous TiO_2 solar cells have been well investigated,[23,24,32,33] but research on the inverted cell structure, such as perovskite-sensitized p-type mesoporous NiO, is just beginning.[34−36] Although the research objects in this work are liquid-electrolyte-based p-type solar cells and their stability is inferior to that of solid-state devices, the uncovered working principles are still worth learning to design an efficient interface of perovskites/semiconductors in solid-state p-type solar cells. Besides, in practice, the iodine-based liquid electrolyte used for these p-type perovskite-sensitized NiO solar cells allows them to be very easily combined with conventional n-DSCs to construct efficient p−n tandem solar cells.

RESULTS AND DISCUSSION

Figure 1 shows the cross-section view and top view SEM images of a $CH_3NH_3PbI_3$-sensitized mesoporous NiO film. The NiO film thickness and the concentration of the spin-coating precursor have been optimized to 1.4 ± 0.1 μm and 0.85 mol L^{-1} and are correlated to the solar cell performance (Figure S1 and Table S1, Supporting Information). The phase purity of as-deposited $CH_3NH_3PbI_3$ has been checked by XRD. From Figure 1, it is clear that no $CH_3NH_3PbI_3$ capping layer is present on top of the mesoporous NiO film and the pore channels of the NiO film have not been blocked by $CH_3NH_3PbI_3$. These observations are consistent with the typical feature of mesoscopic solar cells, just like conventional DSCs and QDSCs. That is, the perovskite sensitizers should be in the form of an extremely thin shell or isolated QDs (nanocrystals) or their mixture absorbed on the surface of NiO nanoparticles and play the same role as the dyes in DSCs and QDs in QDSCs. The EDX mapping results clearly show that both "Pb" and "I" elements are homogeneously distributed at different depths of the NiO film, reflecting a good penetration of the $CH_3NH_3PbI_3$ precursor and a homogeneous distribution of the nanocrystalline $CH_3NH_3PbI_3$ sensitizer inside the mesoporous NiO film. The yellow line in Figure 1a highlights the region of the compact NiO layer between the mesoporous NiO film and the FTO-coated glass substrate. Such a layer with a thickness of about 50−80 nm was prepared by spray pyrolysis of an acetonitrile solution of (acetylacetone)nickel.[18,19] For

more details about the compact NiO layer, see Figure S2 in the Supporting Information.

Figure 2 compares the current density−voltage (J−V) curves of the $CH_3NH_3PbI_3$-sensitized NiO solar cells with and without

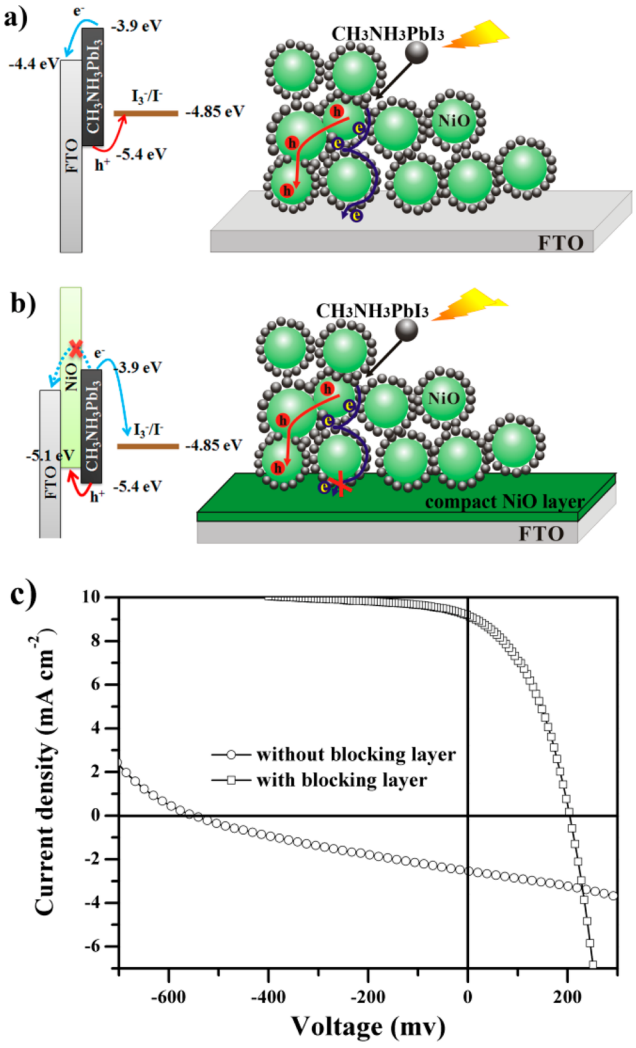

Figure 2. Schematic of the current flow directions in NiO solar cells sensitized by $CH_3NH_3PbI_3$ (a) without and (b) with a compact NiO blocking layer. The insets on the left are the corresponding energy level alignments. (c) J−V curves of $CH_3NH_3PbI_3$-sensitized NiO solar cells with (□) and without (○) the compact NiO blocking layer.

the compact NiO blocking layer. It is quite interesting that the current flow directions are opposite in the two compared solar cells. This phenomenon is quite similar to that of the previously reported CdS/CdSe-sensitized NiO solar cells,[18,19] but $CH_3NH_3PbI_3$ as demonstrated is a more efficient sensitizer than CdS/CdSe; therefore, in both n-type and p-type cells, the detected J_{sc} values in Figure 2 are notably higher than those in the literature.[18,19] For the solar cell without the compact NiO blocking layer, n-type behavior of such a cell is evident: J_{sc} is −2.54 mA cm^{-2}, and the open-circuit photovoltage (V_{oc}) is −548 mV. A photocurrent is suggested to be generated due to electron diffusion along the continuous shell-like layer of $CH_3NH_3PbI_3$ to FTO (Figure 2a). The photovoltage is mostly dependent on the quasi Fermi level of $CH_3NH_3PbI_3$/FTO and the I_3^-/I^- redox potential of the electrolyte. In such a case, NiO nanoparticles may act as the scaffold, just like the insulated Al_2O_3 nanoparticles in the solid-state mesoscopic perovskite solar cell reported by Snaith et al.[26] The hole injection from $CH_3NH_3PbI_3$ to NiO possibly coexists in such a system; however, since the hole diffusion coefficient in the mesoporous NiO network (D = ~10^{-7} cm^2 s^{-1}, as demonstrated later in this work) should be much smaller than that of electron diffusion in $CH_3NH_3PbI_3$ (D = 10^{-2} cm^2 s^{-1}),[27] the bare FTO substrate will collect more electrons than the holes due to successful kinetic competition. For the solar cell with a compact NiO blocking layer, a photocurrent is generated due to photo-injected hole collection through the mesoporous NiO network, while the electron transport path from $CH_3NH_3PbI_3$ to FTO is blocked (Figure 2b). This function of the compact NiO layer is quite similar to that of the NiO buffer layers (hole transfer layer) in organic solar cells, which can selectively collect photogenerated charges.[37] As a consequence, V_{oc} of such a p-type solar cell is 205 mV, which is consistent with its theoretical value determined by the valence band of NiO (−5.1 eV versus vacuum) and redox couple potential of the electrolyte (−4.85 eV for I_3^-/I^-).[7,12]

Figure 3a shows the J−V characteristics of the best $CH_3NH_3PbBr_3$- and $CH_3NH_3PbI_3$-sensitized NiO solar cells under exposure to 100 mW cm^{-2} AM 1.5G simulated sunlight. J_{sc} of the $CH_3NH_3PbI_3$/NiO solar cell is 9.47 mA cm^{-2}, which is much higher than 6.21 mA cm^{-2} of the $CH_3NH_3PbBr_3$/NiO solar cell. The V_{oc} values of the two solar cells are 205 mV ($CH_3NH_3PbI_3$) and 212 mV ($CH_3NH_3PbBr_3$). They are similar because both are determined by the valence band of NiO and redox potential of the electrolyte. The fill factors are 0.36 and 0.40, yielding efficiencies of 0.71 and 0.53, respectively. All of these performance parameters are summarized in Table 1 with those of the best reported p-DSCs and p-QDSCs for comparison. There is a dramatic increase in J_{sc} and therefore the solar conversion efficiency when the organic dyes or inorganic QD sensitizers are replaced by $CH_3NH_3PbI_3$ (Table 1), which is mostly due to the broader light absorption range of $CH_3NH_3PbI_3$ and minimal loss in the charge injection/collection processes as will be demonstrated later. The V_{oc} values of the perovskite-sensitized NiO solar cells are ~200 mV, also higher than those of most of the previously reported p-DSCs based on NiO and the I_3^-/I^- electrolyte (~100 mV, Table 1). IPCE spectra of the perovskite-sensitized NiO solar cells are shown in Figure 3b. The spectral range for the $CH_3NH_3PbI_3$/NiO solar cell is obviously wider than that for the $CH_3NH_3PbBr_3$/NiO solar cell, which can explain their J_{sc} difference. The IPCE maxima are more than 50% for both cells, which is very high in p-type solar cells.[10,13] A further increase of the IPCE maximum is strongly limited by the intrinsic absorption of the NiO film, which absorbs a considerable part of the incident solar cell in competition with the sensitizers but almost makes no photocurrent contribution to the device.[11] For the $CH_3NH_3PbI_3$/NiO solar cell, generation of the photocurrent starts at 800 nm, which is in good agreement with the band gap of $CH_3NH_3PbI_3$ (1.55 eV).[22] For the $CH_3NH_3PbBr_3$/NiO solar cell, it is unexpected that the photocurrent response threshold will reach 650 nm. If calculating from the band gap of $CH_3NH_3PbBr_3$ (2.2 eV), the threshold should be 560 nm, as demonstrated in the previous literature.[22,32] By repeating the experiments, we confirmed that this was not caused by measurement error. It should be caused by the iodine-based electrolyte used in this work, which was different from the previously reported solid-state hole transport material or the bromine-based electrolyte.[32,38] After electrolyte

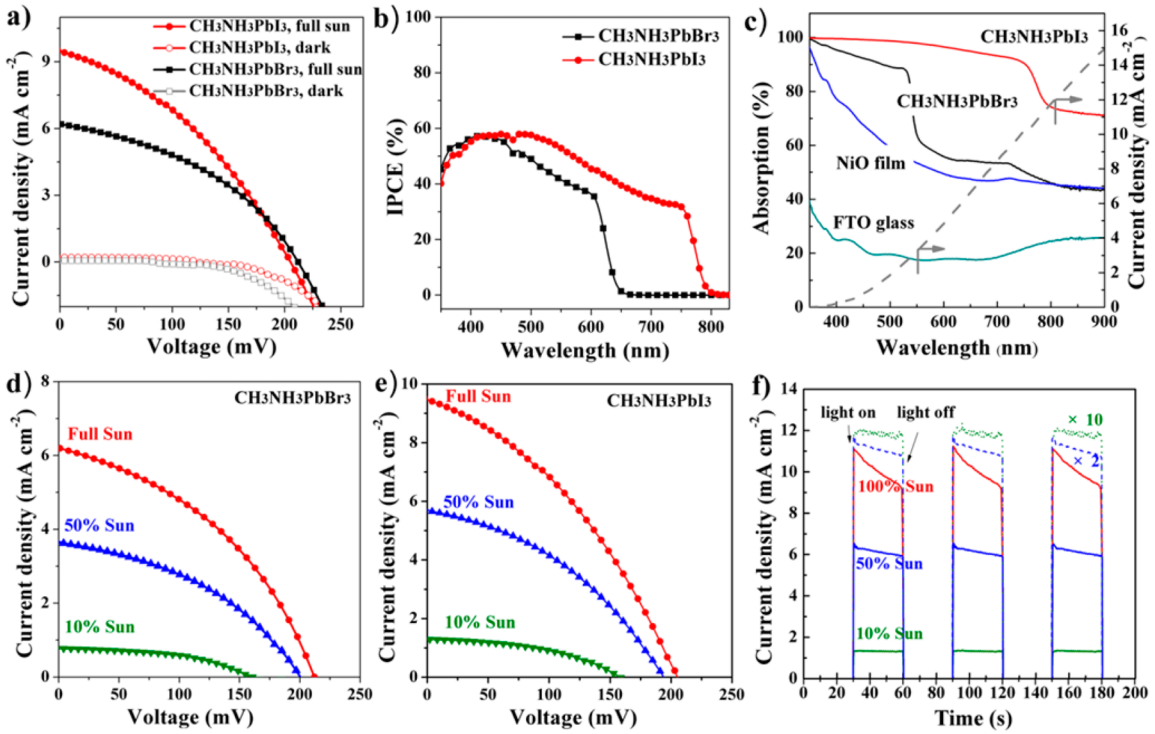

Figure 3. Photovoltaic device characterization: (a) $J-V$ curves and (b) IPCE spectra of perovskite-sensitized NiO solar cells. (c) Light absorption spectra of bare FTO glass, a 1.4 μm thick NiO film on FTO, and perovskite-sensitized NiO films. The right y axis is the calculated current density assuming 100% light harvesting of perovskites minus the intrinsic light absorption of NiO. $J-V$ curves of (d) $CH_3NH_3PbBr_3$- and (e) $CH_3NH_3PbI_3$-sensitized NiO solar cells at different light intensities. (f) Photocurrent response of $CH_3NH_3PbI_3$-sensitized NiO photocathodes to on−off circles of illumination.

Table 1. Performance Comparison between the Solar Cells Studied in the Present Work and the Best Reported p-DSCs and p-QDSCs

sensitizer	electrolyte	V_{oc} (mV)	J_{sc} (mA cm^{-2})	fill factor	η (%)	ref
C343 dye	I^-/I^{3-}	71	1.89	0.39	0.05	10
P1 dye		84	5.48	0.34	0.15	
PMI-6T-TPA dye	I^-/I^{3-}	218	5.35	0.35	0.41	11
		185	7.0	0.33	0.43	13
Se QDs	I_3^-/I^-	318	3.73	0.29	0.34	17
CdS QDs	S_n^{2-}/S^{2-}	111	0.1	0.22		20
CdS/CdSe QDs	S_n^{2-}/S^{2-}	86	0.87	0.32	0.24	18
$CH_3NH_3PbI_3$ (1 sun)	I_3^-/I^-	205	9.47	0.36	0.71	present work
$CH_3NH_3PbI_3$ (0.5 sun)	I_3^-/I^-	192	5.73	0.39	0.86	present work
$CH_3NH_3PbI_3$ (0.1 sun)	I_3^-/I^-	156	1.32	0.45	0.91	present work
$CH_3NH_3PbBr_3$ (1 sun)	I_3^-/I^-	212	6.21	0.40	0.53	present work
$CH_3NH_3PbBr_3$ (0.5 sun)	I_3^-/I^-	200	3.64	0.42	0.61	present work
$CH_3NH_3PbBr_3$ (0.1 sun)	I_3^-/I^-	161	0.78	0.52	0.65	present work

filling to complete the solar cell fabrication, the iodine-based electrolyte may induce an ion exchange reaction between I^- in the electrolyte and $CH_3NH_3PbBr_3$ on the NiO surface, leading to the formation of a new sensitizer, $CH_3NH_3PbBr_{3-x}I_x$. The band gaps of $CH_3NH_3PbBr_{3-x}I_x$ can be successively tuned from 2.2 to 1.5 eV depending on its composition as reported in the literature.[38] Therefore, the sensitizer in the performance-stabilized $CH_3NH_3PbBr_3$/NiO solar cell should actually be $CH_3NH_3PbBr_{3-x}I_x$ with a narrower band gap than $CH_3NH_3PbBr_3$, responsible for the abnormal IPCE spectrum.

Figure 3c compares the UV−vis absorption of the bare FTO glass and a 1.4 μm thick mesoporous NiO film on FTO glass before and after perovskite sensitization. The absorption thresholds of $CH_3NH_3PbBr_3$- and $CH_3NH_3PbI_3$-sensitized NiO films are 560 and 800 nm, respectively, consistent with the literature.[32,38] The absorption of $CH_3NH_3PbBr_3$- and $CH_3NH_3PbI_3$-sensitized NiO films is over 90% in the whole light absorption range, reflecting the close to saturated light-harvesting efficiency (LHE) of these photocathodes, which are a prerequisite for the realization of high J_{sc} values of the corresponding solar cells.[11] Furthermore, from Figure 3c, we can clearly see that the useless light absorption by the NiO film occupies a considerable fraction of incident solar light (30−40%). If assuming that all of the remaining incident solar light (despite absorption by the NiO film and FTO glass) can be harvested by the light absorber, we can predict a theoretical J_{sc} as a function of the light absorption threshold by integrating with the AM 1.5G solar photon flux. The result is shown on the

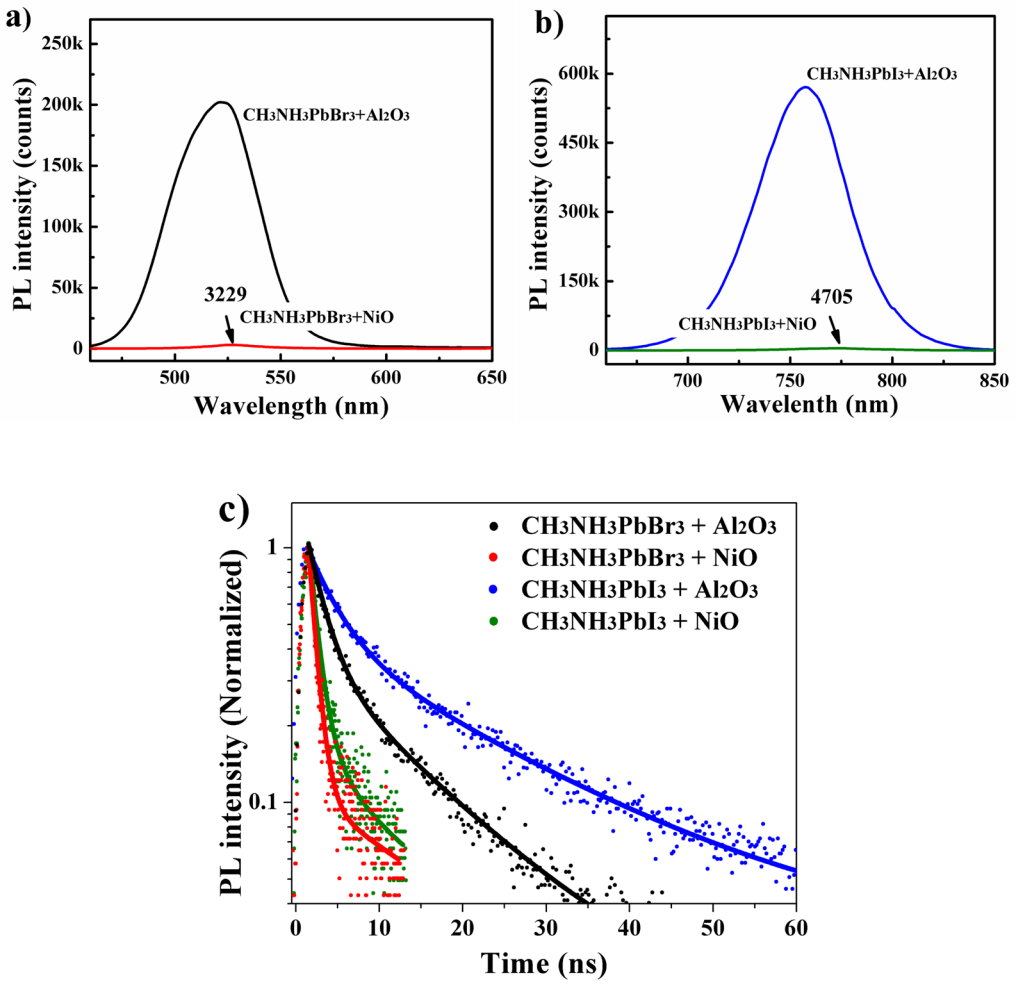

Figure 4. Photoluminescence of (a) $CH_3NH_3PbBr_3$ and (b) $CH_3NH_3PbI_3$ on mesoporous Al_2O_3 and NiO films. (c) Time-resolved photoluminescence of the perovskites on mesoporous Al_2O_3 and NiO films. The symbols are the measurement results. The solid lines are two-exponential fits.

right *y* axis in Figure 3c. It can be found that the predicted J_{sc} for a 800 nm threshold light absorber, such as $CH_3NH_3PbI_3$ in this case, should be ~12 mA cm^{-2} and that for a 560 nm threshold light absorber, such as $CH_3NH_3PbBr_3$, should be ~3.5 mA cm^{-2}. The latter cannot explain the measured J_{sc} of ~6.0 mA cm^{-2} for the $CH_3NH_3PbBr_3$/NiO solar cell, but considering the real light absorption threshold of $CH_3NH_3PbBr_{3-x}I_x$ (650 nm), a calculated J_{sc} of 6.5 mA cm^{-2} matches well with the actually measured J_{sc}. The real tested high J_{sc} values are very close to the theoretically calculated J_{sc} values , reflecting that the internal quantum efficiency regarding the hole injection and collection processes in these perovskite-sensitized NiO solar cells should be very high.[11]

Parts d and e of Figure 3 show the *J*−*V* curves of the perovskite-sensitized NiO solar cells under illumination of different light intensities (0.1, 0.5, and 1 sun). Figure 3f shows the photocurrent response of the $CH_3NH_3PbI_3$/NiO solar cell to on−off circles of illumination. Both of the solar cells present nonlinear dependences of J_{sc} on the light intensity (see Table 1). This phenomenon is suggested to result from the mass diffusion limitation of the electrolyte. To decrease the solvation effect on perovskites, ethyl acetate is used instead of the typical acetonitrile as the solvent of the iodine electrolyte, which indeed leads to much more stable devices (see Table S2 in the Supporting Information),[33] but the disadvantage is that the ionic diffusion coefficient of I_3^- could be much lower in ethyl acetate than that in acetonitrile.[39] The time-resolved photocurrent responses in Figure 3f strongly support this point. When the shutter starts to open (light on), the peak photocurrent of the solar cell can be observed because of the higher concentration of I_3^- already present surrounding the perovskites, which is enough to regenerate the reduced perovskites after their photoexcitation and hole injection to NiO. Subsequently, the concentration of I_3^- inside the NiO mesopores begins to decrease due to slow mass transfer of the I_3^-/I^- couples in the electrolyte. Therefore, the photocurrents decrease continuously. As the light intensity is reduced, the variation in photocurrents also decreases due to less I_3^- ions being required to regenerate excited perovskites.[40] As a consequence of the nonlinear dependence of J_{sc} on the light intensity, the solar conversion efficiency of the solar cells at lower light intensity is even higher; the best is 0.91%, achieved by the $CH_3NH_3PbI_3$/NiO solar cell under 0.1 sun of illumination (Table 1).

Figure 4 shows the static photoluminescence (PL) and time-resolved PL characterization results on the perovskite-sensitized NiO films using the perovskite-modified mesoporous Al_2O_3 films with similar light absorption as the references. The mesoporous Al_2O_3 film was used because its band energy levels prevent interfacial charge (both electron and hole) injection

from the perovskites;[41] besides, the mesoporous structure similar to that of the NiO film could provide similar growth conditions of the perovskite nanocrystals inside the mesopores. From Figure 4a,b, it can be observed that the PL peak intensity at about 525 nm for the $CH_3NH_3PbBr_3$/NiO sample is significantly quenched by a factor of 62.5 when compared to that of the $CH_3NH_3PbBr_3/Al_2O_3$ sample, and the PL peak intensity at about 765 nm for the $CH_3NH_3PbI_3$/NiO sample is significantly quenched by a factor of 121 when compared to that of the $CH_3NH_3PbI_3/Al_2O_3$ sample. Similar to a lot of previous literature on DSCs and QDSCs, such a high degree of PL quenching should originate from fast charge transfer from the photoexcited sensitizer to the semiconductor at their mesoscopic interface.[41−43] More exactly, in this work, it should be due to the hole injection from the photoexcited perovskites to the valence band of NiO, which is allowed due to their appropriate energy level alignment.

To better understand the hole injection process, the time-resolved PL spectra have been measured, as shown in Figure 4c. Two exponential decays are required to fit the time-resolved PL data. For the $CH_3NH_3PbI_3/Al_2O_3$ and $CH_3NH_3PbBr_3/Al_2O_3$ samples, the lifetimes, quoted as the time taken to reach 1/e of the initial PL intensity, are 8.20 and 3.95 ns, respectively. The lifetime of 8.20 ns for the $CH_3NH_3PbI_3/Al_2O_3$ sample is consistent with the PL lifetimes of the pure $CH_3NH_3PbI_3$ thin films reported previously.[26−28] For the $CH_3NH_3PbI_3$/NiO and $CH_3NH_3PbBr_3$/NiO samples, the lifetimes are greatly reduced to 1.09 and 0.87 ns, respectively. According to eq 1,[26−28] the

$$\phi_{inj} = 1 - \frac{\tau_{perovskite/NiO}}{\tau_{perovskite/Al_2O_3}} \quad (1)$$

hole injection efficiency (Φ_{inj}) can be estimated from the lifetimes (τ) to be as high as 87% and 78% for the $CH_3NH_3PbI_3$/NiO and $CH_3NH_3PbBr_3$/NiO samples, respectively. As IPCE for the p-type solar cell could be expressed by IPCE = (LHE)$\Phi_{inj}\eta_{cc}$ (charge collection efficiency), a high hole injection efficiency Φ_{inj} is important to explain the tested high IPCE of the perovskite solar cells.

Figure 5 represents the collection kinetics of photoinjected holes through the mesoporous NiO networks in the p-type solar cells, tested by the transient photocurrent/photovoltage decay methods. The kinetics should be governed by the well-known trapping−detrapping mode. Figure 5a compares the hole lifetimes (τ_r) in NiO before recombination with the reduced I^- in the electrolyte and the hole transport time (τ_t) through the 1.4 μm thick mesoporous NiO film. Figure 5b shows their hole diffusion coefficients (D) calculated by $D = d^2/2.35\tau_t$, where d is the actual film thickness of 1.4 μm.[33] The τ_r values in these perovskite-sensitized NiO solar cells are very close to those reported previously in p-DSCs.[10,44−46] The hole diffusion coefficients are also in the low range of 10^{-7}−10^{-6} $cm^2\ s^{-1}$, similar to those for the reported p-DSCs,[10,44−46] but in contrast to electron diffusion coefficients for the TiO_2 network of n-DSCs (typically in the range of 10^{-5}−10^{-4} $cm^2\ s^{-1}$).[33] These results reflect that the hole transport and recombination kinetics do not change so much with the sensitizer type (organic dyes or perovskites) and are mostly related to the intrinsic properties of the NiO network and the NiO/electrolyte interface. A similar conclusion could be found for the $CH_3NH_3PbI_3$-sensitized TiO_2 photoelectrochemical cells reported recently,[33] though the electron and hole transport inside the perovskites could be very fast.[30] Figure 5c shows relatively high (>70%) charge collection efficiencies (η_{cc}) of the perovskite-sensitized solar cells, defined as $\eta_{cc} = 1 - \tau_t/\tau_r$.[33] The much thinner optimized thickness of the NiO film in the perovskite-sensitized solar cells (1.4 μm) than in the conventional p-DSCs (typically 2−3 μm) should be a benefit, because the shortened hole transport path will result in a shorter τ_t, which is associated with the much higher light absorption coefficients of the perovskites than the organic dyes.[22−26]

CONCLUSION

In conclusion, we have for the first time demonstrated decently high efficiency of liquid-electrolyte-based p-type solar cells by sensitization of $CH_3NH_3PbBr_3$ and $CH_3NH_3PbI_3$ on NiO nanocrystals. The notable J_{sc} of 9.41 mA cm^{-2} and efficiency of 0.71% have been achieved by the $CH_3NH_3PbI_3$/NiO solar cell at 1 sun of light intensity. The success is achieved on the basis of the following obstacles being resolved by this work: (1) the compact NiO blocking layer deposited by spray pyrolysis holds the key to the "p-type" current flow in the perovskite-sensitized NiO solar cells; (2) the correct selection of perovskite sensitizers, which are specific for the p-type solar cells, guaranteeing the high hole injection efficiency at the perovskite/NiO interface and the high hole collection efficiency through the mesoporous NiO network. Note that, to date, among the kinds of dyes, quantum dots, or extremely thin absorbers in the sensitization-type solar cells, the perovskites are the only sensitizers which can work efficiently on both the n-type TiO_2 photoanode and p-type NiO photocathode. Although, in the current state, it is still hard to dtermine the general principle for designing efficient inorganic sensitizers (beyond the "donor−acceptor" dyes) for the p-type photocathode, this work at least presents a successful example. The bipolar charge transport property (both high mobility and long lifetime of electrons and holes) of the perovskites may play the key role. Furthermore, the limitations on further increasing the J_{sc} of p-type solar cells have also been clarified in this work: (1) The intrinsic light absorption of NiO wastes a considerable part of solar light. In view of the fact that the $CH_3NH_3PbI_3$-sensitized TiO_2 solar cell with the same electrolyte has achieved a J_{sc} of 15−18 mA cm^{-2},[33] such disadvantageous light absorption of NiO should be the biggest loss of our p-type solar cells, which could be resolved by alternative p-type semiconductors with better optical transparency as we reported before.[44−46] (2) The electrolyte diffusion limitation imposes a restriction on the J_{sc} of p-type solar cells at higher light intensity, which might be resolved by optimization of the pore structure of the photocathode and the electrolyte composition. After resolution of the above-mentioned problems, perovskite-sensitized p-type solar cells with further elevated J_{sc} values are highly desired, and their combination with conventional dye-sensitized n-type half-cells by sharing the common iodine electrolyte to construct highly efficient p−n tandem cells should be very promising. The related works are ongoing in our laboratory.

EXPERIMENTAL SECTION

Fabrication of Perovskite-Sensitized NiO Photocathodes and Solar Cells. All chemicals unless otherwise noted were of analytical grade and were used as received. First, a compact thin layer of NiO was deposited on FTO glass (8 Ω $square^{-1}$, Nippon Sheet Glass, Japan) by spray pyrolysis of 0.2 mol L^{-1} nickel acetylacetonate in acetonitrile at 500 °C.[18,19] The mesoporous NiO film was then

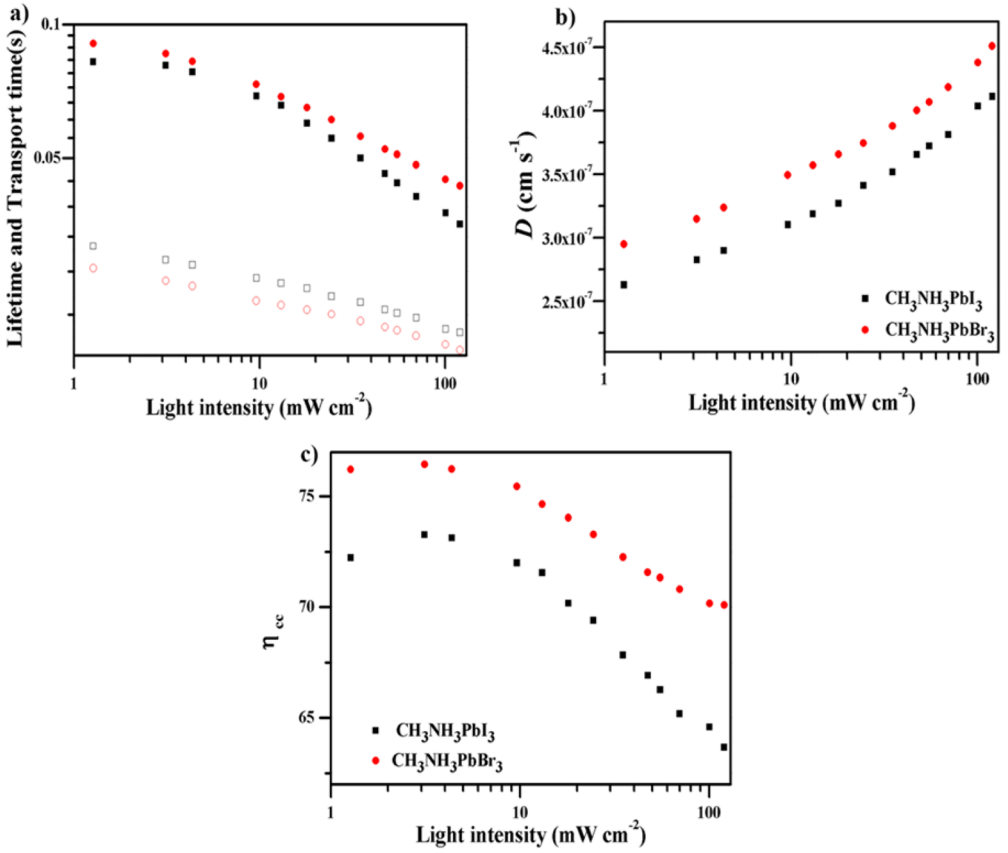

Figure 5. Dependences of the (a) hole lifetime and transport time, (b) hole diffusion coefficient (D), and (c) charge collection efficiency (η_{cc}) on the light intensity of the perovskite-sensitized NiO solar cells.

deposited on top of the compact layer by screen-printing using a paste composed of commercial NiO nanoparticles (20 nm, Inframat, United States), which was subsequently annealed at 450 °C for 30 min and 550 °C for 15 min. Before the perovskite deposition, a bright yellow $CH_3NH_3PbI_3$ solution and a colorless $CH_3NH_3PbBr_3$ solution were prepared by dissolving 1.157 g of PbI_2 and 0.395 g of CH_3NH_3I in 2.95 mL of γ-butyrolactone and 0.278 g of CH_3NH_3Br and 0.921 g of $PbBr_2$ in 2.95 mL of DMF at 60 °C overnight. Afterward, the mesoporous NiO films were spin-coated with the perovskite solutions at 2000 rpm for 30 s in a dry environment (air atmosphere, humidity <30%), followed by heating at 100 °C for 15 min until the dark gray color of $CH_3NH_3PbI_3$ and the orange color of $CH_3NH_3PbBr_3$ appeared.

Catalytic counter electrodes were prepared by pyrolysis of a H_2PtCl_6 solution (120 μg cm^{-2}) on FTO glasses using a hot-wind gun set at 400 °C for 20 min. The perovskite-sensitized NiO photocathodes were sandwiched together with the platinized counter electrodes and sealed with a hot-melt polymer gasket (25 μm, Surlyn). The electrolyte composed of 0.5 M LiI, 0.25 M I_2, 0.3 M *tert*-butylpyridine, and 0.03 M urea in ethyl acetate was injected into the cell through a drilled hole via the vacuum backfilling technique.

Characterization. *General Materials Characterization.* The morphology of the NiO film was observed using a field emission scanning electron microscope (FEI-Sirion 200, FEI). The film thickness was measured by a profilometer (Dektak 150, Veeco Instruments Inc.). UV/vis−NIR spectra of the films were recorded on a PerkinElmer UV/vis spectrophotometer (model Lambda 950).

Photovoltaic Characterization. A 450 W xenon light source solar simulator (Oriel, model 9119) with an AM 1.5G filter (Oriel, model 91192) was used to give an irradiance of 100 mW cm^{-2}. The light intensity was tuned by different mesh grids and calibrated with a standard silicon reference cell. The current−voltage characteristics of the cell under these conditions were obtained by applying an external potential bias to the cell and measuring the generated photocurrent with a Keithley model 2400 digital source meter (Keithley, United States). The active area for solar cell measurement was determined by a 4 × 4 mm^2 mask to prevent scattered light. A similar data acquisition system was used to control the IPCE measurement. A white light bias (1% sunlight intensity) was applied to the sample during the IPCE measurements in the ac mode (10 Hz). The static photoluminescence and time-resolved photoluminescence characterizations were done on an Edinburg PLS 920 (Edinburg Co. Ltd.). Transient photovoltage/photocurrent decay measurements were done on a homemade photoelectrochemical system. A white light bias on the sample was generated from an array of diodes. Red light pulse diodes (0.05 s square pulse width, 100 ns rise and fall time) controlled by a fast solid-state switch were used as the perturbation source. The voltage dynamics were recorded on a PC-interfaced Keithley 2602A source meter with a 100 μs response time. The perturbation light source was set to a suitably low level for the voltage decay kinetics to be monoexponential. By varying the white light bias intensity, the recombination rate constant and hole diffusion rate constant could be estimated over a range of applied biases.

■ ASSOCIATED CONTENT

Ⓢ Supporting Information

UV−vis results, J−V curves of the $CH_3NH_3PbI_3$-sensitized NiO solar cells achieved at different NiO film thicknesses, SEM image of the NiO compact layer, and transient photocurrent/photovoltage decays of the $CH_3NH_3PbI_3$/NiO solar cells. This material is available free of charge via the Internet at http://pubs.acs.org.

■ AUTHOR INFORMATION

Corresponding Author

*E-mail: wnlochenwei@mail.hust.edu.cn.

Author Contributions

[⊥]H.W. and X.Z. contributed equally to this work.

Notes

The authors declare no competing financial interest.

■ ACKNOWLEDGMENTS

We express our sincere thanks for the financial support by the National Natural Science Foundation (Grants 21103058, 21173091, and 20903030), 973 Program of China (Grant 2011CBA00703), Basic Scientific Research Funds for Central Colleges (Grants 2012YQ027 and 2013TS040), and Beijing Key Laboratory for Sensors of the Beijing Information Science & Technology University (Grant KF20131077208). We also thank the Analytical and Testing Center of the Huazhong University Science & Technology for the sample measurements.

■ REFERENCES

(1) O'Regan, B.; Grätzel, M. A Low-Cost High-Efficiency Solar Cell Based on Dye-Sensitized Colloidal TiO_2 Films. *Nature* **1991**, *353*, 737−740.

(2) Yella, A.; Lee, H. W.; Tsao, H. N.; Yi, C.; Chandiran, A. K.; Nazeeruddin, M. K.; Diau, E. W. G.; Yeh, C. Y.; Zakeeruddin, S. M.; Grätzel, M. Porphyrin-Sensitized Solar Cells with Cobalt (II/III)-Based Redox Electrolyte Exceed 12% Efficiency. *Science* **2011**, *334*, 629−634.

(3) Hagfeldt, A.; Boschloo, G.; Sun, L.; Kloo, L.; Pettersson, H. Dye-Sensitized Solar Cells. *Chem. Rev.* **2010**, *110*, 6595−6663.

(4) Odobel, F.; Pleux, L. L.; Pellegrin, Y.; Blart, E. New Photovoltaic Devices Based on the Sensitization of p-Type Semiconductors: Challenges and Opportunities. *Acc. Chem. Res.* **2010**, *43*, 1063−1071.

(5) Odobel, F.; Pellegrin, Y.; Gibson, E. A.; Hagfeldt, A.; Smeigh, A. L.; Hammarström, L. Recent Advances and Future Directions To Optimize the Performances of p-Type Dye-Sensitized Solar Cells. *Coord. Chem. Rev.* **2012**, *256*, 2414−2423.

(6) Odobel, F.; Pellegrin, Y. Recent Advances in the Sensitization of Wide-Band-Gap Nanostructured p-Type Semiconductors. Photovoltaic and Photocatalytic Applications. *J. Phys. Chem. Lett.* **2013**, *4*, 2551−2564.

(7) Gibson, E. A.; Smeigh, A. L.; Pleux, L. L.; Hammarström, L.; Odobel, F.; Boschloo, G.; Hagfeldt, A. Cobalt Polypyridyl-Based Electrolytes for p-Type Dye-Sensitized Solar Cells. *J. Phys. Chem. C* **2011**, *115*, 9772−9779.

(8) Qin, P.; Zhu, H.; Edvinsson, T.; Boschloo, G.; Hagfeldt, A.; Sun, L. Design of an Organic Chromophore for p-Type Dye-Sensitized Solar Cells. *J. Am. Chem. Soc.* **2008**, *130*, 8570−8571.

(9) Qin, P.; Linder, M.; Brinck, T.; Boschloo, G.; Hagfeldt, A.; Sun, L. High Incident Photon-to-Current Conversion Efficiency of p-Type Dye-Sensitized Solar Cells Based on NiO and Organic Chromophores. *Adv. Mater.* **2009**, *21*, 2993−2996.

(10) Li, L.; Gibson, E. A.; Qin, P.; Boschloo, G.; Gorlov, M.; Hagfeldt, A.; Sun, L. Double-Layered NiO Photocathodes for p-Type DSSCs with Record IPCE. *Adv. Mater.* **2010**, *22*, 1759−1762.

(11) Nattestad, A.; Mozer, A. J.; Fischer, M. K. R.; Cheng, Y.-B.; Mishra, A.; Bäuerle, P.; Bach, U. Highly Efficient Photocathodes for Dye-Sensitized Tandem Solar Cells. *Nat. Mater.* **2010**, *9*, 31−35.

(12) Powar, S.; Daeneke, T.; Ma, M. T.; Fu, D.; Duffy, N. W.; Götz, G.; Weidelener, M.; Mishra, A.; Buerle, P.; Spiccia, L.; Bach, U. Highly Efficient p-Type Dye-Sensitized Solar Cells Based on Tris(1,2-diaminoethane)cobalt(II)/(III) Electrolytes. *Angew. Chem., Int. Ed.* **2013**, *125*, 630−633.

(13) Powar, S.; Wu, Q.; Weidelener, M.; Nattestad, A.; Hu, Z.; Mishra, A.; Bäuerle, P.; Spiccia, L.; Cheng, Y.-B.; Bach, U. Improved Photocurrents for p-Type Dye-Sensitized Solar Cells Using Nano-Structured Nickel(II) Oxide Microballs. *Energy Environ. Sci.* **2012**, *5*, 8896−8900.

(14) Ji, Z.; He, M.; Huang, Z.; Ozkan, U.; Wu, Y. Photostable p-Type Dye-Sensitized Photoelectrochemical Cells for Water Reduction. *J. Am. Chem. Soc.* **2013**, *135*, 11696−11699.

(15) Li, L.; Duan, L.; Wen, F.; Li, C.; Wang, M.; Hagfeldt, A.; Sun, L. Visible Light Driven Hydrogen Production from a Photo-Active Cathode Based on a Molecular Catalyst and Organic Dye-Sensitized p-Type Nanostructured NiO. *Chem. Commun.* **2012**, *48*, 988−990.

(16) He, J.; Lindström, H.; Hagfeldt, A.; Lindquist, S.-E. Dye-Sensitized Nanostructured Tandem Cell-First Demonstrated Cell with a Dye-Sensitized Photocathode. *Sol. Energy Mater. Sol. Cells* **2000**, *62*, 265−273.

(17) Qian, J.; Jiang, K.-J.; Huang, J.-H.; Liu, Q.-S.; Yang, L.-M.; Song, Y. A Selenium-Based Cathode for a High-Voltage Tandem Photoelectrochemical Solar Cell. *Angew. Chem., Int. Ed.* **2012**, *124*, 10497−10500.

(18) Safari-Alamuti, F.; Jennings, J. R.; Hossain, M. A.; Yung, L. Y. L.; Wang, Q. Conformal Growth of Nanocrystalline CdX (X = S, Se) on Mesoscopic NiO and Their Photoelectrochemical Properties. *Phys. Chem. Chem. Phys.* **2013**, *15*, 4767−4774.

(19) Chan, X.-H.; Jennings, J. R.; Hossain, M. A.; Yu, K. K. Z.; Wang, Q. Characteristics of p-NiO Thin Films Prepared by Spray Pyrolysis and Their Application in CdS-Sensitized Photocathodes. *J. Electrochem. Soc.* **2011**, *158*, H733−H740.

(20) Shalom, M.; Hod, I.; Tachan, Z.; Buhbut, S.; Tirosh, S.; Zaban, A. Quantum Dot Based Anode and Cathode for High Voltage Tandem Photo-Electrochemical Solar Cell. *Energy Environ. Sci.* **2011**, *4*, 1874−1878.

(21) Kang, S. H.; Zhu, K.; Neale, N. R.; Frank, A. J. Hole Transport in Sensitized CdS−NiO Nanoparticle Photocathodes. *Chem. Commun.* **2011**, *47*, 10419−10421.

(22) Rhee, J. H.; Chung, C.-C.; Diau, E. W.-G. A Perspective of Mesoscopic Solar Cells Based on Metal Chalcogenide Quantum Dots and Organometal-Halide Perovskites. *NPG Asia Mater.* **2013**, *5*, e68.

(23) Burschka, J.; Pellet, N.; Moon, S.-J.; Humphry-Baker, R.; Gao, P.; Nazeeruddin, M. K.; Grätzel, M. Sequential Deposition as a Route to High-Performance Perovskite-Sensitized Solar Cells. *Nature* **2013**, *499*, 316−319.

(24) Kim, H.-S.; Lee, C.-R.; Im, J.-H.; Lee, K.-B.; Moeh, T.; Marchioro, A.; Moon, S.-J.; Humphry-Baker, R.; Yum, J.-H.; Moser, J. E.; Grätzel, M.; Park, N.-G. Lead Iodide Perovskite Sensitized All-Solid-State Submicron Thin Film Mesoscopic Solar Cell with Efficiency Exceeding 9%. *Sci. Rep.* **2012**, *2*, 591.

(25) Liu, M.; Johnston, M. B.; Snaith, H. J. Efficient Planar Heterojunction Perovskite Solar Cells by Vapour Deposition. *Nature* **2013**, *501*, 395−398.

(26) Lee, M. M.; Teuscher, J.; Miyasaka, T.; Murakami, T. N.; Snaith, H. J. Efficient Hybrid Solar Cells Based on Meso-Superstructured Organometal Halide Perovskites. *Science* **2012**, *338*, 643−647.

(27) Stranks, S. D.; Eperon, G. E.; Grancini, G.; Menelaou, C.; Alcocer, M. J. P.; Leijtens, T.; Herz, L. M.; Petrozza, A.; Snaith, H. J. Electron-Hole Diffusion Lengths Exceeding 1 Micrometer in an Organometal Trihalide Perovskite Absorber. *Science* **2013**, *342*, 341−344.

(28) Xing, G.; Mathews, N.; Sun, S.; Lim, S. S.; Lam, Y. M.; Grätzel, M.; Mhaisalkar, S.; Sum, T. C. Long-Range Balanced Electron- and Hole-Transport Lengths in Organic-Inorganic $CH_3NH_3PbI_3$. *Science* **2013**, *342*, 344−347.

(29) Heo, J. H.; Im, S. H.; Noh, J. H.; Mandal, T. N.; Lim, C.-S.; Chang, J. A.; Lee, Y. H.; Kim, H.-j.; Sarkar, A.; Nazeeruddin, M. K.; Grätzel, M.; Seok, S. I. Efficient Inorganic−Organic Hybrid Heterojunction Solar Cells Containing Perovskite Compound and Polymeric Hole Conductors. *Nat. Photonics* **2013**, *7*, 486−491.

(30) Marchioro, A.; Teuscher, J.; Friedrich, D.; Kunst, M.; Krol, R.; Moehl, T.; Grätzel, M.; Moser, J.-E. Unravelling the Mechanism of Photoinduced Charge Transfer Processes in Lead Iodide Perovskite Solar Cells. *Nat. Photonics* **2014**, *8*, 250−255.

(31) Liu, D.; Kelly, T. L. Perovskite Solar Cells with a Planar Heterojunction Structure Prepared Using Room-Temperature Solution Processing Techniques. *Nat. Photonics* **2014**, *8*, 133−138.

(32) Kojima, A.; Teshima, K.; Shirai, Y.; Miyasaka, T. Organometal Halide Perovskites as Visible-Light Sensitizers for Photovoltaic Cells. *J. Am. Chem. Soc.* **2009**, *131*, 6050−6051.
(33) Zhao, Y.; Zhu, K. Charge Transport and Recombination in Perovskite $(CH_3NH_3)PbI_3$ Sensitized TiO_2 Solar Cells. *J. Phys. Chem. Lett.* **2013**, *4*, 2880−2884.
(34) Jeng, J.-Y.; Chen, K.-C.; Chiang, T.-Y.; Lin, P.-Y.; Tsai, T.-D.; Chang, Y.-C.; Guo, T.-F.; Chen, P.; Wen, T.-C.; Hsu, Y.-J. Nickel Oxide Electrode Interlayer in $(CH_3NH_3)PbI_3$ Perovskite/PCBM Planar-Heterojunction Hybrid Solar Cells. *Adv. Mater.* **2014**, *26*, 4107−4113.
(35) Wang, Q.; Shao, Y.; Dong, Q.; Xiao, Z.; Yuan, Y.; Huang, J. Large Fill-Factor Bilayer Iodine Perovskite Solar Cells Fabricated by Low-Temperature Solution-Process. *Energy Environ. Sci.* **2014**, *7*, 2359−2365.
(36) Wang, K.-C.; Jeng, J.-Y.; Shen, P.-S.; Chang, Y.-C.; Diau, E-W-G.; Tsai, C.-H.; Chao, T.-Y.; Hsu, H.-C.; Lin, P.-Y.; Chen, P.; Guo, T.-F.; Wen, T.-C. p-Type Mesoscopic Nickel Oxide/Organometallic Perovskite Heterojunction Solar Cells. *Sci. Rep.* **2014**, DOI: 10.1038/srep04756.
(37) Irwin, M. D.; Buchholz, D. B.; Hains, A. W.; Chang, R. P. H.; Marks, T. J. p-Type Semiconducting Nickel Oxide as an Efficiency-Enhancing Anode Interfacial Layer in Polymer Bulk-Heterojunction Solar Cells. *Proc. Natl. Acad. Sci. U.S.A.* **2008**, *105*, 2783−2787.
(38) Noh, J. H.; Im, S. H.; Heo, J. H.; Mandal, T. N.; Seok, S. I. Chemical Management for Colorful, Efficient, and Stable Inorganic−Organic Hybrid Nanostructured Solar Cells. *Nano Lett.* **2013**, *13*, 1764−1769.
(39) Hauch, A.; Georg, A. Diffusion in the Electrolyte and Charge-Transfer Reaction at the Platinum Electrode in Dye-Sensitized Solar Cells. *Electrochim. Acta* **2001**, *46*, 3457−3466.
(40) Lee, K.-M.; Chiu, W.-H.; Hsu, C.-Y.; Cheng, H.-M.; Lee, C.-H.; Wu, C.-G. Ionic Liquid Diffusion Properties in Tetrapod-like ZnO Photoanode for Dye-Sensitized Solar Cells. *J. Power Sources* **2012**, *216*, 330−336.
(41) Lu, H.-P.; Mai, C.-L.; Tsia, C.-Y.; Hsu, S.-J.; Hsieh, C.-P.; Chiu, C.-L.; Yeh, C.-Y.; Diau, E. W.-G. Design and Characterization of Highly Efficient Porphyrin Sensitizers for Green See-Through Dye-Sensitized Solar Cells. *Phys. Chem. Chem. Phys.* **2009**, *11*, 10270−10274.
(42) Chang, Y.-C.; Wu, H.-P.; Reddy, N. M.; Lee, H.-W.; Lu, H.-P.; Yeh, C.-Y.; Diau, E. W.-G. The Influence of Electron Injection and Charge Recombination Kinetics on the Performance of Porphyrin-Sensitized Solar Cells: Effects of the 4-*tert*-Butylpyridine Additive. *Phys. Chem. Chem. Phys.* **2013**, *15*, 4651−4655.
(43) Koops, S. E.; O'Regan, B. C.; Barnes, P. R. F.; Durrant, J. R. Parameters Influencing the Efficiency of Electron Injection in Dye-Sensitized Solar Cells. *J. Am. Chem. Soc.* **2009**, *131*, 4808−4818.
(44) Xiong, D.; Xu, Z.; Zeng, X.; Zhang, W.; Chen, W.; Xu, X.; Wang, M.; Cheng, Y.-B. Hydrothermal Synthesis of Ultrasmall $CuCrO_2$ Nanocrystal Alternatives to NiO Nanoparticles in Efficient p-Type Dye-Sensitized Solar Cells. *J. Mater. Chem.* **2012**, *22*, 24760−24768.
(45) Xiong, D.; Zhang, W.; Zeng, X.; Xu, Z.; Chen, W.; Cui, J.; Wang, M.; Sun, L.; Cheng, Y.-B. Enhanced Performance of p-Type Dye-Sensitized Solar Cells Based on Ultrasmall Mg-Doped $CuCrO_2$ Nanocrystals. *ChemSusChem* **2013**, *6*, 1432−1437.
(46) Xu, Z.; Xiong, D.; Wang, H.; Zhang, W.; Zeng, X.; Ming, L.; Chen, W.; Xu, X.; Cui, J.; Wang, M.; Powar, S.; Bach, U.; Cheng, Y.-B. Remarkable Photocurrent of p-Type Dye-Sensitized Solar Cell Achieved by Size Controlled $CuGaO_2$ Nanoplates. *J. Mater. Chem. A* **2014**, *2*, 2968−2976.